JOURNAL OF MATERIALS SCIENCE 17 (1982) 1745–1752

Failure mechanisms and acoustic emission amplitude distributions in automotive finishes

J. ROOUM, R. D. RAWLINGS
Department of Metallurgy and Materials Science, Imperial College of Science and Technology, Prince Consort Road, London SW7 2BP, UK

A complete automotive finish consists of a steel substrate with a phosphate coat and three paint coats. The complete finish and several sub-systems of the finish have been tested in tension and the acoustic emission monitored. The results of the acoustic emission, complemented with information from other techniques, such as scanning electron microscopy, have enabled the identification of a number of failure mechanisms and the strain ranges over which they occur. Analysis of the amplitude distributions in terms of overlapping Lorentzian peaks has demonstrated that each failure mechanism is associated with emissions of a characteristic amplitude.

1. Introduction

The paint finish on a car is a complex system consisting of several coatings which differ in thickness, chemical composition, structure and mechanical properties. The complete system usually consists of a steel substrate, a phosphate coat and three paint coats.

The phosphate coat is a thin layer of a mixed iron and zinc phosphate, known as phosphophyllite, with overlaying needles of zinc phosphate (hopeite). The phosphate layer inhibits the spread of underflim corrosion and is thought to improve the adhesion of the substrate to the primer.

The first paint coat is an electrocoat primer. That is, it is applied electrolytically by placing the car in a tank and applying a voltage such that the resin and pigment particles of the paint are attracted to it. The car is usually the anode.

A "surfacer" paint coat is then applied to level out any imperfections and finally a "top-coat" paint coat is applied. The surfacer is either an epoxy ester or an oil-free alkyd resin with additions to fill the imperfections. The top-coat is either a thermoplastic or thermosetting resin.

The top-coat is the main contributor to the appearance of the finish, giving the colour and gloss, but the behaviour and protective properties of the finish depend on all the coats and their compatibility.

The paint industries use many mechanical and physical techniques [1] to determine the properties of paint finishes during their development and the monitoring of mechanical tests with acoustic emission may serve to provide additional useful information. Several studies have been reported [2–5] where automobile finishes have been monitored but little effort has been made to relate the acoustic emission to failure processes within the paint system. We have shown that the acoustic emission arises from loss of adhesion and from micro- and macrocracking in the paint coats and in the phosphate layer. In addition, it is established that the amplitude distributions can be analysed as a series of peaks with each peak characterizing a particular source of the acoustic emission.

2. Experimental procedure

2.1. Materials

Mild steel panels were de-greased and phosphated using the Granodine 16S treatment, which gives a zinc phosphate with a coating weight of 2.6 g^{-2}. They were then given a chromium rinse (Deoxylite 76) and three paint coats were applied, namely an anodic electrocoat primer, an oil-free alkyd resin surfacer and a melamine formaldehyde thermosetting resin topcoat. After the application of each coat several panels were retained for testing. Panels were produced with the finish either on both sides or on just one side.

0022–2461/82/061745–08$03.46/0

2.2. Tensile testing and acoustic emission

The panels were cut into strips (15 mm x 80 mm x 0.7 mm) and tensile tested in an Instron machine at a strain rate of 4×10^{-4} sec^{-1}, to selected strains and to fracture of the steel. Each test was repeated at least five times.

During testing the acoustic emission was monitored using a lead zirconium titanate (PZT) transducer (Dunegan Endevco model D140 BDE, resonant frequency 150 kHz) coupled to the midpoint of the specimen with a spring-clip, through a thin layer of vacuum grease. The resulting signal was pre-amplified (gain 40 dB) and the ring-down counts (total gain 93 dB), event counts and amplitude distributions were obtained using standard equipment supplied by Dunegan Endevco and Acoustic Emission Consultants.

For each system, photographs were taken during the test, using a cold flashlight, and at intervals of about 2% strain, to give a record of the gross surface damage.

2.3. Post test examination

The adhesion of the various paint finishes as a function of strain was investigated using cross-hatch tests [1]. A grid of lines about 0.5 mm apart was scored through the coatings; then sellotape was attached and pulled off rapidly. The appearance of the grid at the end of the procedure allowed the adhesion of the finishes to be compared.

The surfaces of the specimens before and after testing were examined in a Cambridge scanning electron microscope (SEM). Specimens were also examined in cross-section after mounting in Araldite and polishing with diamond paste.

3. Results

3.1. Acoustic emission

The acoustic emission characteristics, e.g., strain dependence and form of amplitude distribution, were very similar for a given system, whether coated on one or both sides. Only the number of counts differed, being about double for the system coated on both sides. These two types of specimens will not be differentiated in the following text.

The events against strain curves for the systems tested are shown in Fig. 1. Although there are large variations in the number of events for a given system, the differences between systems can be readily detected. The strain ranges during which the acoustic activity was most marked can be deduced from Fig. 1, but they are more clearly

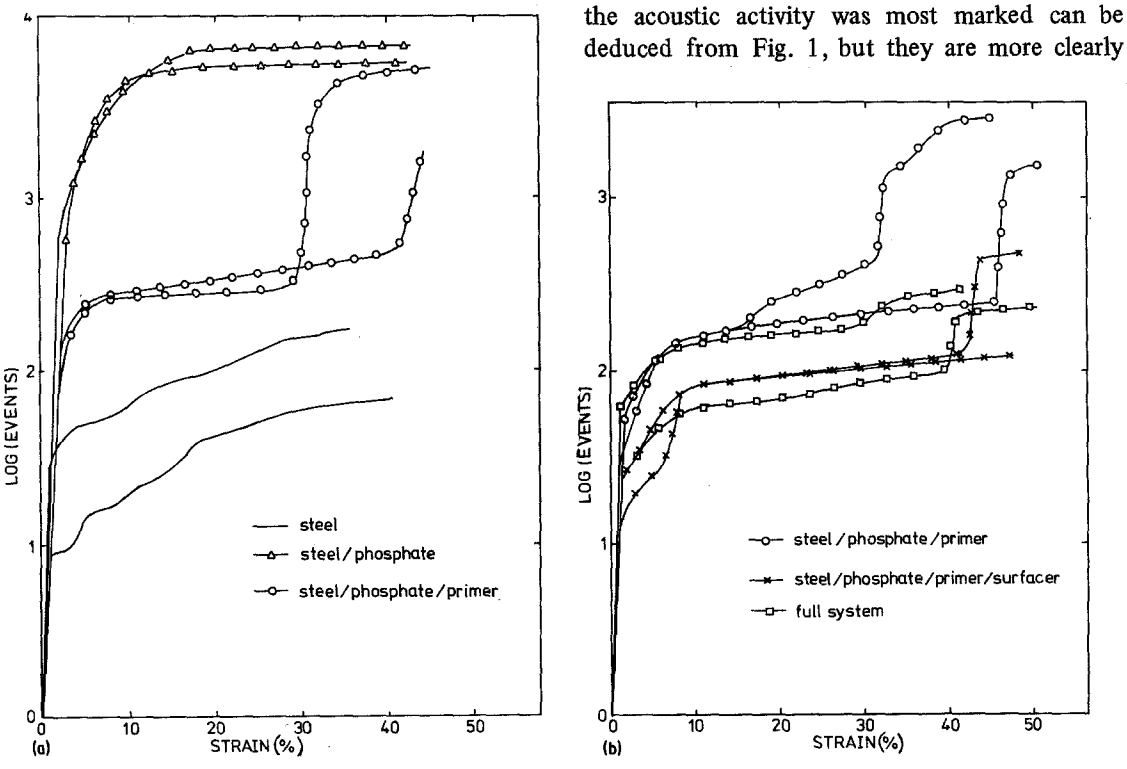

Figure 1 The accumulative event count as a function of strain. The two curves for each system represent the maximum and minimum recorded. (a) Coated both sides; (b) coated one side.

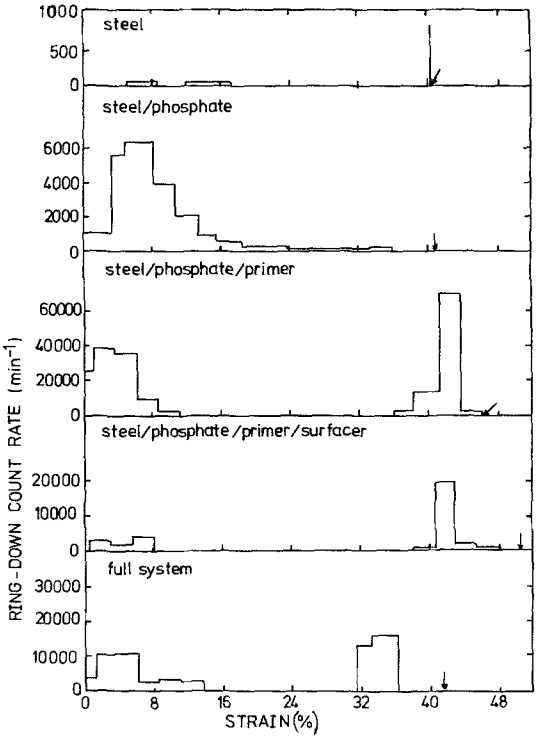

Figure 2 Typical plots of the ring-down count-rate as a function of strain, showing the strain ranges over which there was acoustic activity. The arrows mark the fracture strain. All specimens coated on both sides except the full system and steel/phosphate/primer/surfacer.

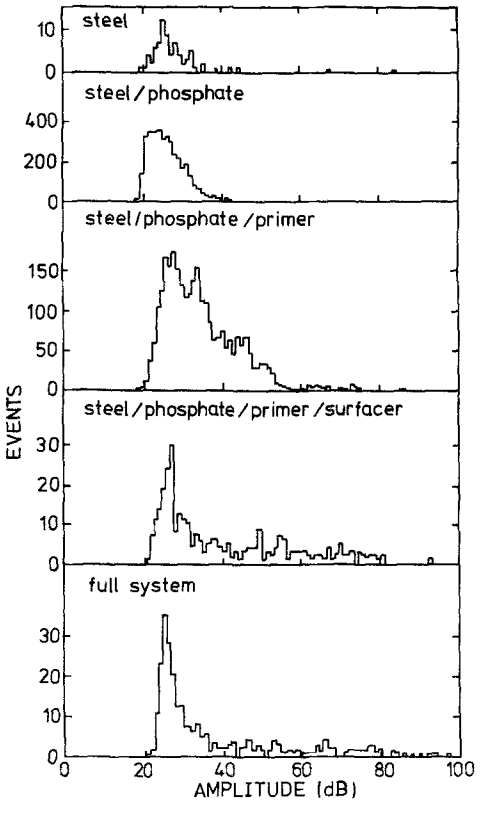

Figure 3 Typical amplitude distributions at failure (full system and steel/phosphate/primer/surfacer coated on one side only).

shown in the ring-down count-rate against strain curves (see Fig. 2). Steel and steel with a phosphate coat exhibited only one peak in the acoustic emission which occurred at a strain of $< 10\%$. The other systems in which paint coats were present showed two peaks, one at strain $< 10\%$ and one at strain $> 30\%$. The limited amount of published information is consistent with these results. For example, the reported [2] strain dependence of the ring-down count-rate for a cathodic electrocoat on a phosphated steel substrate also showed two distinct maxima. Furthermore, Moslé and Wellenkötter [3] found that emissions for a phosphated steel were produced mainly in the early stages of a tensile test.

Amplitude distributions at failure are shown in Fig. 3. The steel and steel/phosphate show emissions with amplitudes only below 40 dB. The addition of further coats resulted in more complex distributions with amplitudes extending to 80 dB. In Fig. 4 amplitude distributions recorded at about 10% strain are compared with those at fracture. It

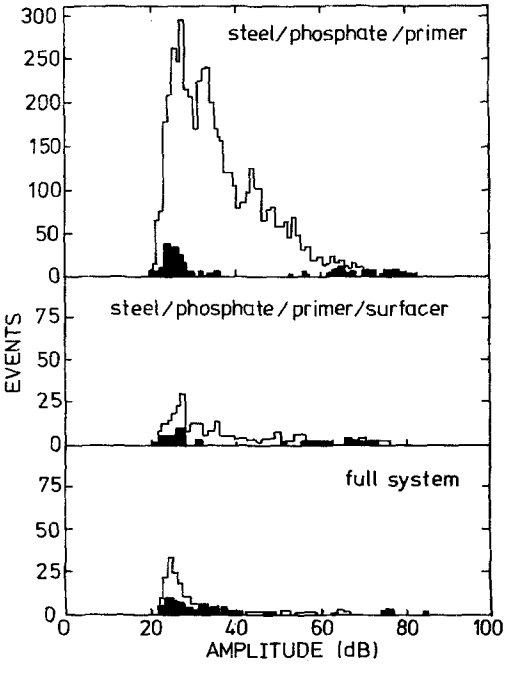

Figure 4 Comparison of typical amplitude distributions at 10% strain (shaded) and at failure (full system and steel/phosphate/primer/surfacer coated on one side only).

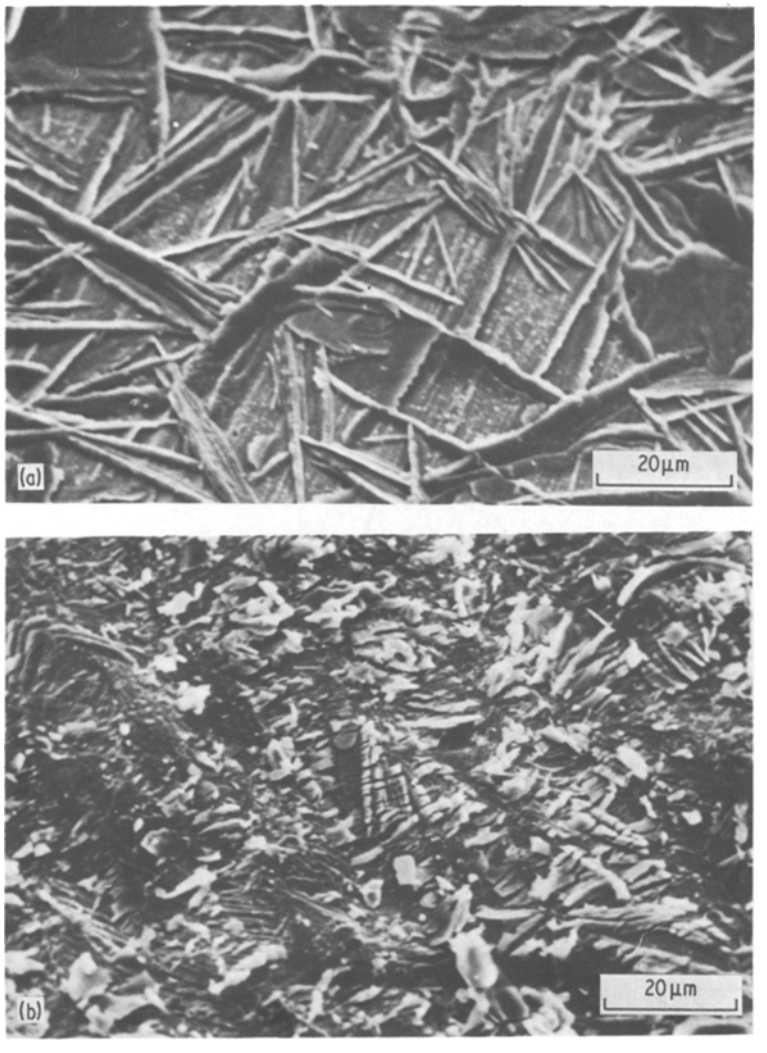

Figure 5 Scanning electron micrographs of the phosphate coat surface. (a) Before testing with many hopeite crystals present; (b) after testing with cracking and detachment of hopeite crystals.

can be seen that the events with amplitudes between 35 and 60 dB were only recorded at the higher strains.

3.2. Failure observations

3.2.1. Observations at low strains (< 10%)

At low strains only the steel/phosphate showed any surface damage. As shown in Fig. 5, many of the hopeite needles were cracked and others had become detached from the phosphophyllite. When studied in cross-section, the various paint coatings could be clearly distinguished but the thin phosphate coating (< 2 μm thick) could not be examined in any detail. Microcracking was seen within all the paint coatings and in all samples. The orientation of the cracks, with respect to the specimen surface and the tensile axis, varied along the specimen but they were largely parallel to each other within a given region. Other forms of cracking were sometimes observed, e.g., the unusual circular cracks near the outer surface of the top-coat (see Fig. 6). At low strains the interfaces between coats acted as crack stoppers and no cracks have been seen running from the outer surface through two or three coats to the steel.

Comparison of cross-hatch tests before testing and at various strains indicated that adhesion loss occurred at low strains for all systems except the complete finish. However, it is considered that adhesion loss did take place in the full system, since it did so in the sub-systems, and that the cross-hatch tests failed to demonstrate the adhesion loss due to the strength and flexibility of the top-coat.

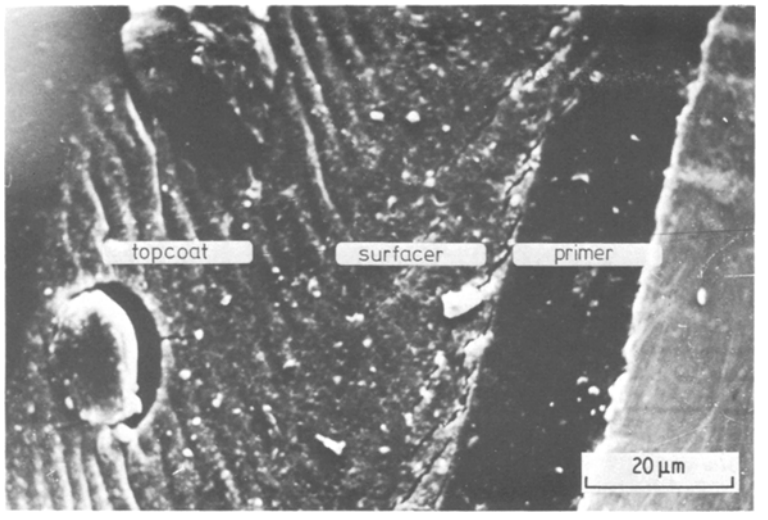

Figure 6 Cross-section through the full system showing the top-coat with unusual circular cracks together with the more common parallel cracks in the top-coat and surfacer.

3.2.2. Observations at higher strains

No difference was noticed in the behaviour of the sub-systems as the strain increased up to $> 30\%$ strain. Visible damage then began to appear on the surfaces of the specimens with paint coatings. As shown in Fig. 7 this consisted of localized peeling of diamond-shaped regions which grew and then cracked perpendicular to the tensile axis. Finally, the coatings cracked across the whole specimen and gross peeling took place.

Electron probe microanalysis of the backs of flakes that had peeled off showed the presence of zinc and SEM revealed uncracked hopeite needles. Zinc was also identified on the exposed surface of the specimens.

4. Discussion

In the case of the steel/phosphate system acoustic activity was only recorded at low strain; the failure modes responsible for the emissions were adhesion loss between the phosphophyllite and the hopeite and cracking of the hopeite needles.

Cross-hatch tests on the specimens with paint coatings showed that adhesion loss occurred at low strains. Examination of the peeled areas suggested that this adhesion loss took place within the phosphate layer and was due mainly to the detachment of hopeite needles from the underlying phosphophyllite. Microcracking of the paint coats was also observed at low strains. The high-strain acoustic emission coincided with the appearance of visible

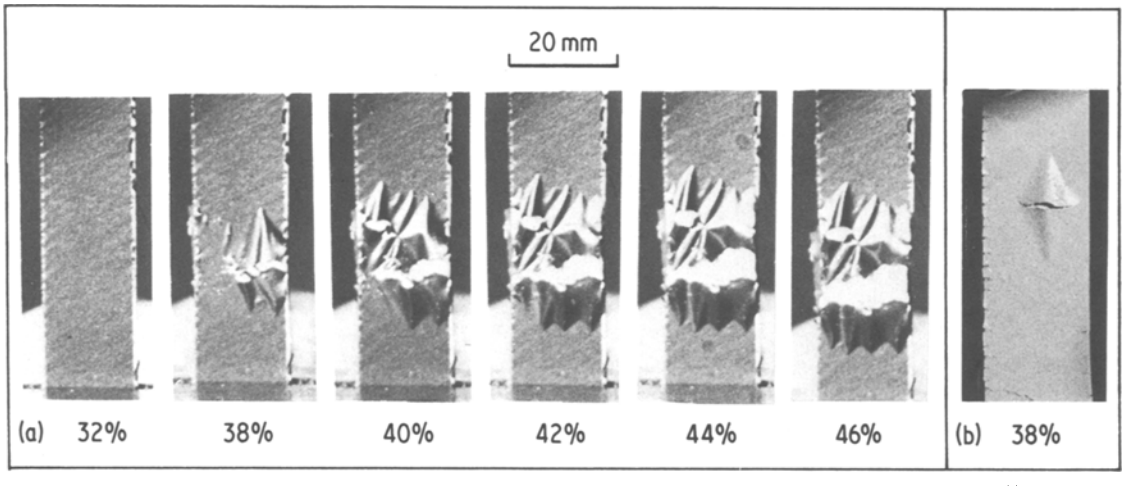

Figure 7 Photographs showing the development of damage in steel/phosphate/primer. (a) Formation of many diamond-shaped defects leading to cracking across the whole width of the specimen; (b) a single diamond-shaped defect which has cracked.

damage on the surface of the specimens [6]. This is shown in Fig. 8 where the strain dependencies of accumulative ring-down count and area of visible damage are presented. It can be seen that there is good correlation between the degree of damage and the ring-down counts.

The amplitude distributions were complex, reflecting the large number of different failure processes. They did not give good fits to the commonly-used power-law distribution [7]. The validity of this characterization is at present being questioned and several other descriptions for the amplitude distributions have been proposed [8, 9]. In this work the distributions consisted of a series of peaks centred about certain amplitudes. It is reasonable that each peak is associated with a particular failure mechanism. If, as is often assumed [10], the acoustic emission energy is proportional to the energy of the source process, then this would imply that the different failure mechanisms are of different energies. In the absence of a generally accepted description for amplitude distributions the peaks here have been taken to conform to a Lorentzian distribution. It is thought that the main results of the following analysis would not be significantly altered if an alternative distribution, for example, Gaussian or Rayleigh, were assumed.

A computer program that distinguished and quantified a series of overlapping Lorentzian peaks was used to analyse the amplitude distributions (except those for untreated steel which gave too few events for a satisfactory analysis). Typical examples of the fit are shown in Fig. 9. The results of the analysis are given in Table I.

The agreement between specimens of a given system was good; only in the case of the steel/phosphate/primer/surfacer was there a variation in the order of the peak intensities; in this case the most frequently occurring order is shown in Table I.

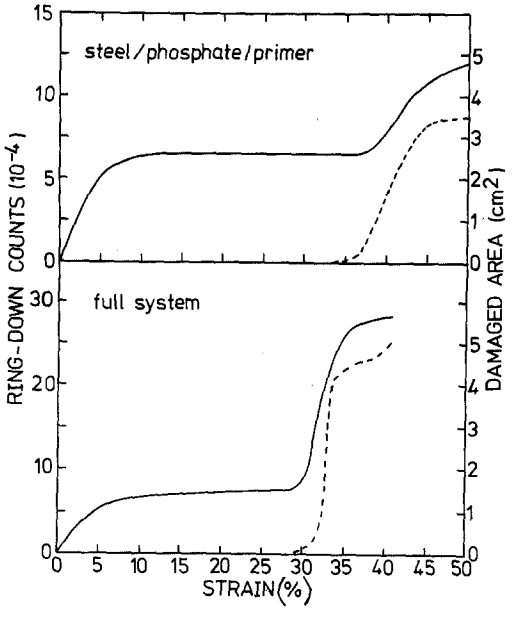

Figure 8 Graphs showing the good correlation between the extent of surface damage, given by the broken curve, and the accumulative ring-down count at high strains.

The results of the analysis indicate that the peaks in the amplitude distributions are centred about 22, 26, 35 and 47 dB with scattered data above 60 dB. It is possible to assign the source failure mechanisms to these peaks in the amplitude distribution as follows:

(a) the 22 dB peak was observed only for the phosphated steel and, hence, must be related to

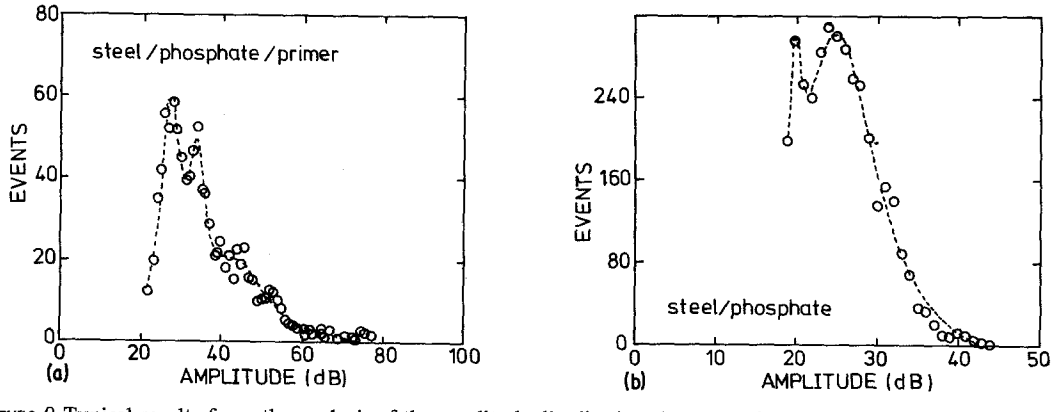

Figure 9 Typical results from the analysis of the amplitude distributions in terms of overlapping Lorentzian peaks. The broken lines represent the computer fit to the experimental data given by the circles. (a) Steel/phosphate/primer; (b) steel/phosphate.

TABLE I Peak positions and intensities of the peaks in the amplitude distributions at 10% strain and failure

Specimen	Measurement point	Intensity*				
		Peak position 22 ± 1 dB	Peak position 26 ± 1 dB	Peak position 35 ± 1 dB	Peak position 47 ± 2 dB	Peak position > 60 dB
Steel/phosphate	10% strain	2*	1			
	Failure	2	1			
Steel/phosphate/primer	10% strain		1			†
	Failure		1	2	3	†
Steel/phosphate/primer/surfacer	10% strain		1			†
	Failure		1	2	3	†
Steel/phosphate/primer/surfacer/top-coat (full system)	10% strain		1	2		†
	Failure		1	2		†
Failure process		Hopeite cracking	Adhesion loss	Peeling and microcracking	Peeling and microcracking	Microcracking

*Key to intensity code: 1, high intensity; 2, medium intensity; 3, low intensity.
†There were insufficient events above 60 dB for the computer program to fit peaks. However, the dagger indicates the presence of a small number of high-amplitude events.

the cracking of hopeite needles which took place only within the steel/phosphate system.

(b) The 26 dB peak appears for all systems at low strains and is attributed to the adhesion failure which occurred within the phosphate layer mainly between the phosphophyllite and hopeite.

(c)The high amplitude emissions (> 60 dB) can be accounted for by the second low-strain failure process, microcracking in the paint coats, which was detected in the low-strain distributions for the systems with paint coats. From Figs 3 and 4 it seems possible that microcracking in the top-coat may give higher amplitude emissions than microcracking in the surfacer.

(d) The peaks at 35 and 47 dB were observed at high strains for systems with paint coatings and are therefore related to the gross damage. This involves loss of adhesion on a sufficient scale to cause the diamond-shaped rucks followed by cracking and peeling. Fig. 4 shows that many events around 26 dB are emitted at high strains and these are attributable to the further loss of adhesion. It follows that the 35 and 47 dB peaks must be associated with the macrocracking and peeling but there is not enough evidence to distinguish between these.

The assignations of the peaks in the amplitude distributions are indicated in Table I. This interpretation has also been found to hold for automotive finishes with differing formulations of phosphates, cathodic primer and after water soaking [11].

5. Conclusions

(a) The various failure mechanisms in the automotive finish when tested in tension have been identified as: (i) cracking of the hopeite crystals (when no paint coat is present), (ii) loss of adhesion between the hopeite and the underlying phosphophyllite, (iii) microcracking in the paint coats, (iv) formation of diamond-shaped rucks, (v) gross peeling and (vi) macrocracking. These mechanisms are not completely independent of one another and in particular Mechanism ii was involved in Mechanism iv.

(b) Acoustic emission occurred in two regions, one below 10% strain and the other at greater than 30% strain. Investigation of the finishes established that Mechanisms i, ii, and iii occurred at low strains whereas Mechanisms iv, v and vi did not take place until a later stage in the test.

(c) Analysis of the amplitude distributions in terms of overlapping Lorentzian peaks showed that each failure mechanism was characterized by events centred around specific amplitudes.

Acknowledgements

The authors would like to thank ICI Paints Division for supplying the test panels and advice, Professor D. Pashley for the research facilities and the SRC for financial support. The authors are indebted to Dr I. Morrison for his assistance with the computer program.

References

1. G. SCHURR, Paint Testing Manual, ASTM SPT 500 (American Society for the Testing of Materials, Philadelphia, 1972).
2. R. D. RAWLINGS and T. A. STRIVENS, *J. Oil Col. Chem. Assoc.* **63** (1980) 412.
3. H. G. MOSLÉ and B. WELLENKÖTTER, *Z. Werkstofftechnik* 9 (1978) 265.
4. *Idem*, Presented at the European Federation of Corrosion Conference on Surface Protection by Organic Coatings, Budapest, May 1979.
5. *Idem*, Presented at the Deutsche Gessellshaft fur Metallkunde Symposium on Acoustic Emission, Bad Nauheim, April 1979.
6. J. S. ROOUM and R. D. RAWLINGS, Presented at the 5th Meeting of the European Working Group on Acoustic Emission, Dortmund, Germany, October 1979.
7. A. POLLOCK, *Non-Destructive Test.* **6** (1973) 264.
8. J. HOLT and A. EVANS, Central Electricity Generating Board Report Number RD/L/N40/76 (1976).
9. K. ONO, *Mater. Eval.* **34** (1976) 177.
10. M. MIRABILE, *Non-Destructive Test* 8 (1975) 77.
11. J. A. ROOUM and R. D. RAWLINGS, to be published.

Received 30 September
and accepted 9 November 1981